Pro-Arrhythmic Effects of Gaseous Pollutants under Healthy Conditions: An In-Silico Study

Laura C. Palacio[1], Javier Saiz[2], Catalina Tobón[1*]

[1]MATBIOM, Universidad de Medellín, Medellín, Colombia
[2]CI[2]B, Universitat Politècnica de València, Valencia, Spain

Abstract

Air pollution is responsible for millions of global deaths annually. The most dangerous gaseous pollutants are sulfur dioxide (SO₂), carbon monoxide (CO), and nitrogen oxides (NOₓ), which have been linked to an increased risk of cardiac arrhythmias. However, the underlying mechanisms have not been fully established in humans. This study uses multiscale atrial models to assess the effects of individual gaseous pollutants at low, medium, and high concentrations. For this, mathematical equations describing the effects of these pollutants were included in an atrial cell model to evaluate the electrophysiological characteristics. Then, the modified cell model was incorporated into a 3D model of human atria to evaluate the propagation dynamics. The results indicate pro-arrhythmic effects in a concentration-dependent manner. SO₂ was the pollutant with the highest effects, achieving an action potential duration decrease and triggering the most chaotic and disordered propagation characterized by several re-entries. In conclusion, gaseous air pollutants, particularly SO₂ and CO at high concentrations, show pro-arrhythmic effects in a concentration-dependent manner.

1. Introduction

Air pollution is responsible for over 6.5 million deaths worldwide each year [1]. Some of the most dangerous gaseous pollutants are sulfur dioxide (SO_2), carbon monoxide (CO), and nitrogen oxides (NO_x), which have been linked to an increased risk of cardiac arrhythmias [2]–[4]. However, the underlying pathophysiological mechanisms remain largely unknown in humans due to the epidemiological nature of most studies. It has been found that SO_2, CO, and NO_x affect different ionic currents, which can impact the action potential and potentially contribute to initiating and maintaining atrial arrhythmias. This study uses multiscale atrial models to assess the effects of individual gaseous pollutants at low, medium, and high concentrations.

2. Methods

Based on experimental data, concentration-dependent equations were developed to simulate the effects of gaseous pollutants on ionic currents. They were incorporated into an atrial cell model and in a 3D model of human atria.

2.1. Models of gaseous pollutants effects and atrial cell model

The Courtemanche model [5] was implemented to simulate the atrial action potential. Based on an experimental study in H9c2 cells derived from rat embryonic cardiomyocytes [6], where the effect of CO was evaluated at a concentration of 1 mM in an ischemic medium for 30 minutes, an effect was found blockage on the L-type calcium current (I_{CaL}) of 44.5%. The half-maximal inhibitory concentration (IC_{50}) value calculated assuming a Hill coefficient (h) equal to 1, was included in the following pore-blocking equation:

$$b_{CO\_CaL} = \frac{1}{1+\left(\frac{1247}{D_{CO}}\right)}, \qquad (2)$$

where D_{CO} is the CO concentration in µM. This equation was introduced on the I_{CaL} equation of the cell model.

Using the Hill equation, we developed concentration-dependent equations to simulate the SO_2 effects on I_{CaL}, sodium (I_{Na}), transient outward (I_{to}) potassium and inward rectifying (I_{K1}) potassium currents. Based on an experimental study [7], the mathematical relationship between the concentration of SO_2 and the blocking factor of I_{CaL} is as follows:

$$b_{SO_2\_CaL} = \frac{1}{1+\left(\frac{35.99}{D_{SO_2}}\right)}, \qquad (3)$$

where D_{SO2} is the SO_2 concentration in µM. The equations relating the increment of I_{Na}, I_{to}, and I_{K1} due to SO_2 were developed according to experimental studies [8], [9] as follows:

$$e_{SO_2\_Na} = \frac{0.841}{1+\left(\frac{10.97}{D_{SO_2}}\right)^{1.07}}, \qquad (4)$$

$$e_{SO_2\_K1} = \frac{0.262}{1+\left(\frac{28.17}{D_{SO_2}}\right)}, \qquad (5)$$

$$e_{SO_2\_to} = \frac{0.374}{1+\left(\frac{16.74}{D_{SO_2}}\right)}, \qquad (6)$$

In agreement with experimental data [10], the mathematical relationship between the concentration of NO_x and the blocking of the current I_{Na} is the following:

$$b_{NO\_Na} = \frac{1}{1+\left(\frac{523}{D_{NO}}\right)^{6.8}}, \qquad (7)$$

where D_{NO} is the NO_x concentration in nM. To simulate the effect of the NO_x on the I_{CaL} current, the Michaelis-Menten equation was implemented as follows:

$$e_{NO\_CaL} = \frac{0.59(D_{NO})}{D_{NO}+0.007}, \qquad (8)$$

where the values 0.59 nM and 0.007 nM are the values of e_{max} and half-maximal effective concentration (EC_{50}) respectively. This equation was fitted using human atrial myocyte data from [11]. The blocking and increasing factors were introduced to the I_{CaL}, I_{Na}, I_{K1}, and I_{to} equations in the cell model, as follows:

$$I_{CaL} = \left(1 - b_{CO\_CaL}\right)(1 - b_{SO_2\_CaL})(1 + e_{NO\_CaL})g_{CaL}dff_{Ca}(V_m - 65), \qquad (9)$$

$$I_{Na} = \left(1 + e_{SO_2\_Na}\right)\left(1 - b_{NO\_Na}\right)g_{Na}m^3hj(V_m - E_{Na}), \qquad (10)$$

$$I_{K1} = \frac{(1 + e_{SO_2\_K1})g_{K1}\,(V_m - E_{K1})}{1 + e^{0.07(V + 80)}}, \qquad (10)$$

$$I_{to} = \left(1 + e_{SO_2\_to}\right)g_{to}oa^3oi(V_m - E_{to}), \qquad (11)$$

The modified model was incorporated into a 3D model of human atria to evaluate the dynamics of propagation.

2.2. 3D model of human atrial

A 3D virtual model of human atria was implemented [12]. The model comprises the main anatomical structures, it is composed of 515010 hexahedral elements with a spatial resolution of 300 μm. It includes realistic fiber orientation, electrophysiological heterogeneity, and anisotropy.

To simulate the cardiac action potential propagation through the 3D model, the monodomain model described by the following reaction-diffusion equation was used:

$$\frac{1}{S_v}\nabla.(D\nabla V_m) = C_m\frac{\partial V_m}{\partial t} + I_{ion} - I_{est}, \qquad (12)$$

where V_m is the transmembrane voltage, C_m is the specific membrane capacitance (100 pF), I_{ion} is the total ionic current that crosses the membrane, I_{stim} is the stimulus current, S_v is the surface/volume ratio and D stands for the conductivity tensor. This equation was numerically solved using the finite element method implemented in the EMOS® software, with a temporal resolution of 0.001 ms.

2.3. Simulation protocol

For single-cell simulations, an S1-S1 stimulation protocol was applied, which consists of a train of rectangular pulses of 2 ms duration and -2,000 pA to generate action potentials at a base cycle length (BCL) of 1000 ms. The APD at 90% of the repolarization (APD_{90}) and the different currents were measured on the 10th beat.

To simulate arrhythmias in the 3D model, an S1-S2-S3 stimulation protocol was applied, where S1 simulates the sinus rhythm as a train of stimuli applied in the sinoatrial node at a BCL of 500 ms. S2 and S3 simulate two ectopic foci composed of 6 stimuli each. S2 is located at the interatrial septum near the coronary sinus and S3 at the posterior wall of the left atrium, in the base of the right pulmonary veins. The first S2 and S3 were applied at coupling intervals that generated a unidirectional block, with cycle lengths selected such that the second stimulus from each focus also generated a unidirectional block. The simulations ran for 5 seconds. To calculate the number of reentries, reentry is defined as the propagation activity that presents 2 or more consecutive turns.

Table 1 shows the concentrations defined for each polluting gas, where the high concentration corresponds to an approximate value of the IC_{50}, the medium is half of the high concentration and the low corresponds to 20% of the high concentration.

Table 1. Gaseous air pollutants concentrations.

Concentration level	[CO]	[SO_2]	[NO_x]
Control	0 μM	0 μM	0 nM
Low	250 μM	8 μM	0.002 nM
Medium	625 μM	20 μM	0.005 nM
High	1250 μM	40 μM	0.01 nM

3. Results

The results of single-cell simulations indicate that individual gaseous pollutants exhibit pro-arrhythmic effects in a concentration-dependent manner by altering the action potential.

Under healthy conditions, as the CO concentration increased, a reduction in the magnitude of the maximum peak of the I_{CaL} current was observed and consequently, a reduction in APD_{90} of 23.6% (Figure 1A).

As the SO_2 concentration increased, APD_{90} was reduced up to 38.8%, also presenting a loss of the dome of the plateau phase (Figure 1B). The above is a consequence of the alterations in the ionic currents, which include a reduction in the magnitude of the maximum peak of the I_{CaL} current, and an increase in the maximum peaks of the I_{Na}, I_{to}, and I_{K1} currents.

Finally, as the NO_x concentration increased, an increase in the magnitude of the maximum peak of the I_{Na} and I_{CaL} currents was observed, an effect opposite to what was observed in the other two gases. This generated a more

pronounced dome in the plateau phase, reaching more positive potential values compared to the control (Figure 1C). APD$_{90}$ did not show significant changes.

The resting potentials do not show significant changes.
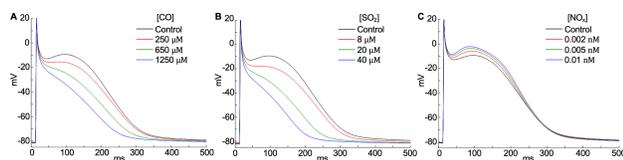
Figure 1. Action potential at control and at low, medium, and high concentrations of each polluting gas (CO, SO$_2$, and NO$_x$).

In the 3D simulations, the main findings showed the existence of reentries, which serve as a trigger for initiating atrial arrhythmias. At the high concentration of CO (Figure 2A), collisions of wavefronts were observed in the center of the posterior wall of both atria. Subsequently, arrhythmic activity began in the left atrium, with transient reentry observed at the base of the left superior pulmonary vein. In the right atrium, the activity was characterized by collision and fragmentation of the wavefront. After ~2900 ms, the arrhythmic activity ended spontaneously.
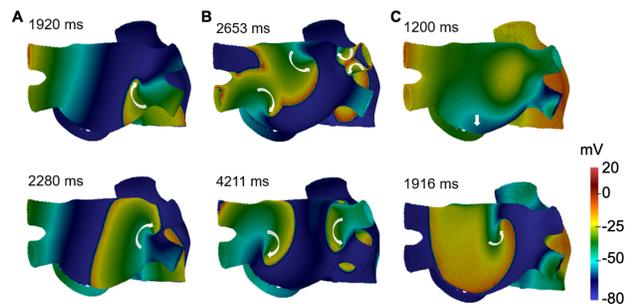
Figure 2. Propagation dynamics in the 3D model at high concentrations of each polluting gases A) CO, B) SO$_2$, and C) NO$_x$. White arrows indicate reentries.

At the high concentration of SO$_2$ (Figure 2B), the generation of 3 re-entries in the left atrium was observed, one in the posterior wall near the left inferior pulmonary vein, and another two anchored to the base of the right superior pulmonary vein. Then multiple reentrant waves (3 to 4 waves at a time) and the generation of a new reentry, which collides simultaneously with the others during the rest of the simulation, gave rise to chaotic activity. In the right atrium, wavefront collisions were observed in the free wall. Starting at ~3000 ms a more irregular activity was observed that gave rise to the generation of a reentry in the terminal crista that subsequently collided at the base of the superior vena cava. Finally, at ~3950 ms a new reentry was generated in the left appendage, and the re-entry located in the terminal crista migrated to the free wall of the atrium.

At the high concentration of NO$_x$ (Figure 2C), shocks of wavefronts were observed in the center of the posterior wall of both atria. Then, the generation of a transient reentry was observed in the left atrium, and at ~2500 ms it ended spontaneously, and the sinus rhythm continued.

SO$_2$ was the pollutant with the highest pro-arrhythmic effects triggering the most chaotic and disordered propagation characterized by a greater number of reentries at high SO$_2$ concentration. Figure 3 shows the number of reentries for each polluting gas at the three concentration levels.
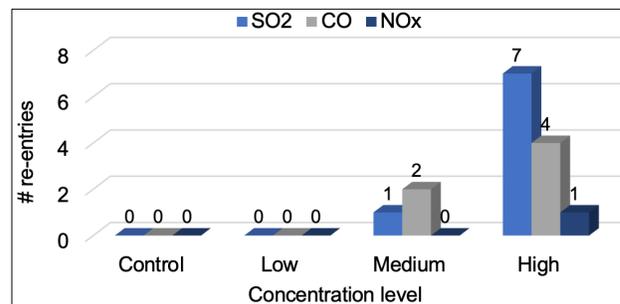
Figure 3. Number of reentries observed for each polluting gas (CO, SO$_2$, and NO$_x$) at low, medium, and high concentrations.

4. Discussion

Epidemiological and experimental studies have demonstrated the proarrhythmic impact of pollutants such as CO, SO$_2$, and NO$_x$.

The simulation results presented in this study indicate that CO may induce a proarrhythmic effect in atrial cardiomyocytes. This effect primarily manifests with a shortened APD, attributable to the concentration-dependent inhibition it exerts on the I$_{CaL}$. In a study conducted on isolated rat atrial and ventricular myocardium [13], a significant APD decrease, diminished contractile strength, and a notable increase in heart rate were observed in response to elevated CO concentrations. Specifically, at a CO concentration of 1000 μM, APD reduction reached approximately 30% compared to the control group. Furthermore, in ventricular myocardial preparations, exogenous CO also resulted in the inhibition of the I$_{CaL}$, leading to a concentration-dependent APD reduction [6].

The simulation results suggest that SO$_2$ is the most proarrhythmic compared to the other pollutants. Particularly at the single-cell level, it had a significant impact on APD. This effect may be attributed to potential changes in the properties of potassium [9] and calcium channels in cardiomyocytes due to SO$_2$ inhalation toxicity [14]. SO$_2$ exposure could potentially harm cardiomyocytes by increasing extracellular potassium and elevating intracellular calcium through ionic channels. Several

studies conducted on rat single-cell ventricular cardiomyocytes investigated the effects of SO_2 derivatives. Zhang et al. [7] observed that SO_2 derivatives had a blocking effect on L-type calcium channels. Furthermore, in experiments with ventricular myocytes isolated from adult rats, inhalation of SO_2 led to an increase in potassium currents I_{to} and I_{K1}, which favored the development of arrhythmias [9]. Additionally, Wei et al. [8] applied a concentration of 10 μM and reported a concentration-dependent increase in the I_{Na} current.

In the context of NO_x, the findings of the present study do not suggest a marked effect on a single-cell scale, with an increase in the potential being observed in the plateau phase. In the 3D model at high concentration, only a single transient reentry event was observed. This limited effect might be explained by the choice of concentrations used in the simulations, which were based on the IC_{50} value from an experimental study. It is possible that higher concentrations of NO_x could result in a more pronounced increase in the I_{CaL}, potentially leading to the emergence of late afterdepolarizations and arrhythmic conditions. Experimental studies [11], [15] have reported that NO_x has the capacity to increase I_{CaL} and I_{Kr} currents. Additionally, Clusin et al. [16] have also reported an effect of NO_x on increasing I_{CaL} current in human atrial myocytes.

5. Conclusion

Our findings suggest that, under healthy conditions, gaseous air pollutants, principally SO_2 and CO at high concentrations, exhibit pro-arrhythmic effects in human atrial models in a concentration-dependent manner.

Acknowledgments

References

[1] R. Fuller *et al.*, "Pollution and health: a progress update," *Lancet Planet. Heal.*, vol. 6, no. 6, pp. e535–e547, Jun. 2022.

[2] L. Andre *et al.*, "Carbon Monoxide Pollution Promotes Cardiac Remodeling and Ventricular Arrhythmia in Healthy Rats," *Am. J. Respir. Crit. Care Med.*, vol. 181, no. 6, pp. 587–595, Mar. 2010.

[3] Y. Hu, T. Wu, X. Liu, and D. Qiao, "Effects of exercise on the cardiovascular function of rats in a sulfur dioxide polluted environment," *An. Acad. Bras. Cienc.*, vol. 94, no. 2, p. e20211180, Jun. 2022.

[4] A. Karoui *et al.*, "Nitrogen Dioxide Inhalation Exposures Induce Cardiac Mitochondrial Reactive Oxygen Species Production, Impair Mitochondrial Function and Promote Coronary Endothelial Dysfunction," *Int. J. Environ. Res. Public Health*, vol. 17, no. 15, pp. 1–14, Aug. 2020.

[5] M. Courtemanche, R. J. Ramirez, and S. Nattel, "Ionic mechanisms underlying human atrial action potential properties: insights from a mathematical model," *Am. J. Physiol.*, vol. 275, no. 1, pp. H301–H321, Jul. 1998.

[6] K. Uemura, S. Adachi-Akahane, K. Shintani-Ishida, and K. Yoshida, "Carbon monoxide protects cardiomyogenic cells against ischemic death through L-type Ca2+ channel inhibition," *Biochem. Biophys. Res. Commun.*, vol. 334, no. 2, pp. 661–668, Aug. 2005.

[7] R.-Y. Zhang *et al.*, "Sulfur dioxide derivatives depress L-type calcium channel in rat cardiomyocytes," *Clin. Exp. Pharmacol. Physiol.*, vol. 38, no. 7, pp. 416–22, Jul. 2011.

[8] H. Wei and Z. Meng, "Enhancing effects of diethyldithiocarbamate on increase of sodium channel by sulfur dioxide derivatives in ventricular myocytes," *Cell Biol. Int.*, vol. 32, no. 9, pp. 1143–1149, Sep. 2008.

[9] A. Nie and Z. Meng, "Sulfur Dioxide Derivative Modulation of Potassium Channels in Rat Ventricular Myocytes," *Arch. Biochem. Biophys.*, vol. 442, no. 2, pp. 187–195, Oct. 2005.

[10] G. Ahmmed, Y. Xu, P. Hong Dong, Z. Zhao, J. Eiserich, and N. Chiamvimonvat, "Nitric oxide modulates cardiac Na+ channel via protein kinase A and protein kinase G," *Circ. Res.*, vol. 89, pp. 1005–1013, 2001.

[11] M. Kirstein, M. Rivet-Bastide, S. Hatem, A. Bénardeau, J. Mercadirer, and R. Fischmeister, "Nitric oxide regulates the calcium current in isolated human atrial myocytes," *J. Clin. Invest.*, vol. 95, no. 2, pp. 794–802, 1995.

[12] A. Ferrer *et al.*, "Detailed Anatomical and Electrophysiological Models of Human Atria and Torso for the Simulation of Atrial Activation," *PLoS One*, vol. 10, no. 11, p. e0141573, Nov. 2015.

[13] D. V Abramochkin, N. N. Haertdinov, M. V Porokhnya, A. L. Zefirov, and G. F. Sitdikova, "Carbon monoxide affects electrical and contractile activity of rat myocardium," *J. Biomed. Sci.*, vol. 18, no. 1, p. 40, 2011.

[14] A. Nie and Z. Meng, "Modulation of L-type Calcium Current in Rat Cardiac Myocytes by Sulfur Dioxide Derivatives," *Food Chem. Toxicol.*, vol. 44, no. 3, pp. 355–363, Mar. 2006.

[15] H. Bae *et al.*, "Effects of Nitric Oxide on Voltage-Gated K+ Currents in Human Cardiac Fibroblasts through the Protein Kinase G and Protein Kinase A Pathways but Not through S-Nitrosylation," *Int. J. Mol. Sci.*, vol. 19, no. 3, p. 814, Mar. 2018.

[16] W. T. Clusin, "Calcium and cardiac arrhythmias: DADs, EADs, and alternans," *Crit. Rev. Clin. Lab. Sci.*, vol. 41, no. 1, p. 115, 2003.

Address for correspondence:

Catalina Tobón Zuluaga
Cra. 87 #30-65, Medellín
ctobon@udemedellin.edu.co